COHERENT REFLECTION AND TRANSMISSION BY A RANDOMLY CRACKED ELASTIC SLAB

Y.C. Angel and A. Bolshakov

Department of Mechanical Engineering and Materials Science
Rice University, MS 321
6100 Main Street
Houston, Texas 77005–1892

INTRODUCTION

The detection of distributed microcracks in metals and of multiple fractures in hydrocarbon reservoirs is of primary importance in the aircraft and oil industries. Often elastic wave methods are used, and detection relies on the choice of an appropriate data processing and interpretation technique.

Data interpretation is difficult because of the lack of a reliable analytical framework describing the interaction between elastic waves and distributed cracks or fractures. Most of the analytical work in this area has focused only on the determination of speed and attenuation, as for example in [1–5], and not on reflection. Yet, reflection is the quantity that can be measured most easily.

In this paper, we review recent results concerning the propagation of SH (antiplane) waves that are either normally or obliquely incident on a random distribution of parallel cracks. In this case, the reflection and transmission on either side of the cracked region are given by simple analytical formulas.

Then, we examine a static approximation in which the cracked region is replaced by a homogeneous equivalent slab. The approximation yields a closed-form formula for the reflection coefficient, in terms of frequency, crack length, crack density, slab thickness, and incident angle. This formula and the earlier analytical formula for the reflection are shown to be in good agreement for near-normal incidence and low frequency. As a result, the closed-form formula can be used as a convenient tool to estimate reflection and to enhance data interpretation at a minimal cost.

THEORY

We consider a linearly elastic, homogeneous, and isotropic unbounded solid that contains a uniform distribution of parallel cracks, as shown in Fig. 1. The cracks have width $2a$, lie in planes orthogonal to the (y_1, y_2) plane, extend to infinity in the $\pm y_3$ directions, and their centers are randomly and uniformly distributed in

Review of Progress in Quantitative Nondestructive Evaluation, Vol 17
Edited by D.O. Thompson and D.E. Chimenti, Plenum Press, New York, 1998

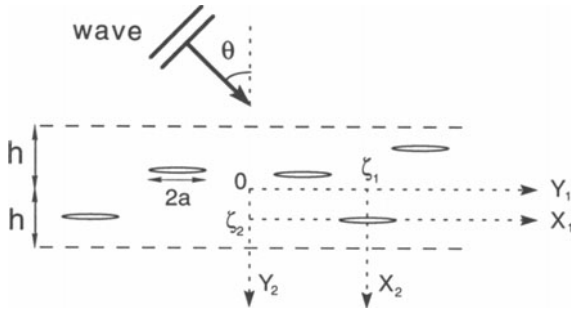

Figure 1. Obliquely incident antiplane wave on a cracked slab of thickness $2h$.

an open slab of width $2h$. The speed c_{T} and the slowness s_{T} of transverse waves in the uncracked solid are given by

$$c_{\mathrm{T}}^2 = \mu/\rho, \quad s_{\mathrm{T}} = 1/c_{\mathrm{T}} \,, \tag{1}$$

where ρ and μ are the mass density and the shear modulus of the solid. An incident antiplane wave propagates toward the cracks at an angle θ relative to the y_2 axis. The displacement u^{inc}, which is in the y_3 direction, is given by

$$u^{\mathrm{inc}}(y_1, y_2) = u_0 \exp\left[ik(y_1 \sin\theta + y_2 \cos\theta)\right], \qquad k = \omega s_{\mathrm{T}}, \tag{2}$$

where the time-harmonic factor, $\exp(-i\omega t)$, is omitted. In (2), u_0 is the amplitude, ω is the frequency, and θ varies in the range $0 \le \theta < \pi/2$.

The incident wave (2) is subjected to multiple reflections between the cracks. We omit throughout this work the factor $\exp(-i\omega t)$, which is common to all field variables in a steady-state regime. Since the distribution of cracks is uniform, the number n of cracks per unit area in the slab is constant on average. We define $\boldsymbol{\zeta} = (\zeta_1, \zeta_2)$ to be the position vector of a crack center and we attach a system of orthogonal axes (x_1, x_2) at $\boldsymbol{\zeta}$, as shown in Fig. 1.

We first consider the case when the wave (2) is incident on N cracks that occupy distinct deterministic positions in a rectangle V_N^h of width $2h$ and length $N/(2hn)$ centered at the origin 0 in Fig. 1. In this case, the total displacement u^{T} in the solid is represented in terms of the incident displacement u^{inc} and of the displacements $\bar{u}^{\mathrm{sc}}$ scattered by the N cracks in the form

$$u^{\mathrm{T}}(y_1, y_2 | \boldsymbol{\Lambda}^N) = u^{\mathrm{inc}}(y_1, y_2) + \sum_{i=1}^{N} \bar{u}^{\mathrm{sc}}(y_1, y_2; \boldsymbol{\zeta}^i | \boldsymbol{\Lambda}^N) \,, \tag{3}$$

where $\boldsymbol{\Lambda}^N = (\boldsymbol{\zeta}^1, \ldots, \boldsymbol{\zeta}^N)$ denotes the configuration of cracks, and the center position $\boldsymbol{\zeta}^i$ after the semi-colon is used to label the displacement scattered by the ith crack. We define the exciting displacement $\bar{u}^{\mathrm{E}}$ on the ith crack as the total displacement minus the ith scattered displacement. Thus, one has

$$\bar{u}^{\mathrm{E}}(y_1, y_2; \boldsymbol{\zeta}^i | \boldsymbol{\Lambda}^N) = u^{\mathrm{T}}(y_1, y_2 | \boldsymbol{\Lambda}^N) - \bar{u}^{\mathrm{sc}}(y_1, y_2; \boldsymbol{\zeta}^i | \boldsymbol{\Lambda}^N). \tag{4}$$

Next, we assume that the N cracks are randomly and uniformly distributed with constant number density n in the rectangle V_N^h. In addition, we assume that

the N parallel cracks have no points of contact and that they are exchangeable. Then, we can define a probability density function $p : \Omega^{2N} \to \mathbb{R}$, where Ω^{2N} is the N-fold Cartesian product of V_N^h, such that the partial integral of p over the $(N-1)$-fold Cartesian product Ω^{2N-2} is equal to n/N. Further, the integral of p over Ω^{2N} is equal to unity.

The average total displacement $< u^{\mathrm{T}} >_N$ in the solid is obtained by multiplying (3) by p, and integrating over Ω^{2N}. In the limit as the number N of cracks tends to infinity, there is an infinite number of cracks that are randomly and uniformly distributed with constant number density n in a slab V_∞^h of width $2h$, as shown in Fig. 1. The average total displacement $< u^{\mathrm{T}} >_\infty$ at any point (y_1, y_2) in the solid can be obtained from (3) in the form

$$< u^{\mathrm{T}} >_\infty (y_1, y_2) = u^{\mathrm{inc}}(y_1, y_2) + n \int_{V_\infty^h} < \bar{u}^{\mathrm{sc}} >_\infty (y_1, y_2; \boldsymbol{\zeta})\, d\boldsymbol{\zeta}. \tag{5}$$

Since the slab extends to infinity in the $\pm y_1$ directions with boundaries parallel to the y_1 axis, and has a uniform distribution of cracks, it follows that the total displacement $< u^{\mathrm{T}} >_\infty (y_1, y_2)$ has the same dependence on y_1 as the incident displacement $u^{\mathrm{inc}}(y_1, y_2)$. Thus, we write

$$< u^{\mathrm{T}} >_\infty (y_1, y_2) =< u^{\mathrm{T}} >_\infty (y_2) \exp(iky_1 \sin\theta). \tag{6}$$

Substituting (6) into (5), applying a symmetry property analogous to (6) to the scattered displacement in the integral of (5), and changing the ζ_1 integration variable that runs along the entire real axis, one finds that

$$< u^{\mathrm{T}} >_\infty (y_2) = u^{\mathrm{inc}}(y_2) + n \int_{V_\infty^h} < \bar{u}^{\mathrm{sc}} >_\infty (0, y_2; \boldsymbol{\zeta})\, d\boldsymbol{\zeta}, \tag{7}$$

where $u^{\mathrm{inc}}(y_2)$ is defined by

$$u^{\mathrm{inc}}(y_2) = u_0 \exp(iky_2 \cos\theta). \tag{8}$$

The average scattered displacement $< \bar{u}^{\mathrm{sc}} >_\infty$ in (7) satisfies two equations that are similar to those of the one-crack problem. The first equation is a second-order Helmholtz differential equation and the second one is a boundary condition that imposes the vanishing of the average total stress $< \sigma_{23}^{\mathrm{T}} >_\infty$ on the crack faces. These equations allow us, as in [6, 7], to write an integral representation for $< \bar{u}^{\mathrm{sc}} >_\infty$ in terms of the average crack-opening displacement.

We now assume that, in a small neighborhood of a fixed crack, the average exciting displacement is equal to the average total displacement (Foldy's assumption). Then, with this assumption, we find from (7) and (8) that the average total displacement has the form

$$\begin{aligned} < u^{\mathrm{T}} >_\infty (y_2) = u_0 \exp(iky_2 \cos\theta) - \\ nBa^2 \int_{-h}^{h} < u^{\mathrm{T}} >'_\infty (\zeta_2)\, \mathrm{sgn}(y_2 - \zeta_2) \exp(ik|y_2 - \zeta_2| \cos\theta)\, d\zeta_2, \end{aligned} \tag{9}$$

where sgn denotes the sign function, and B is a complex-valued number that is defined by

$$Ba^2 = \frac{i}{k \sin\theta} \int_{-a}^{a} b(\nu) \exp(-ik\nu \sin\theta)\, d\nu. \tag{10}$$

The function b in equation (10) is the solution of a singular integral equation and an auxiliary condition, which are given by

$$\int_{-a}^{a} b(\nu)\left[\frac{1}{\nu - x_1} + S(\nu - x_1)\right] d\nu = -\pi \exp(ikx_1 \sin\theta), \qquad |x_1| < a, \tag{11}$$

$$\int_{-a}^{a} b(\nu)\, d\nu = 0. \tag{12}$$

In equation (11), the function S, which is consistent with the radiation condition, is given by

$$S(x) = \int_0^\infty (\frac{\beta}{\xi} - 1)\sin(\xi x)\, d\xi\,, \qquad \beta^2 = \xi^2 - k^2, \qquad \mathrm{Im}(\beta) \le 0, \qquad \mathrm{Re}(\beta) \ge 0\,. \tag{13}$$

Differentiating (9) twice in the range $|y_2| < h$, one finds a second-order ordinary differential equation. The general solution of this equation is

$$< u^{\mathrm{T}} >_\infty (y_2) = C\exp(iKy_2) + D\exp(-iKy_2), \tag{14}$$

where C and D are complex-valued constants and K is a complex-valued wavenumber. The number K is given by

$$K^2 = \bar{K}^2 k^2 \cos^2\theta, \quad \bar{K}^2 = 1/(1 + 2na^2 B). \tag{15}$$

Numerical results in [6, 7] show that $\bar{K}^2$ lies in the upper complex plane for all frequencies. Thus, we can define $\bar{K}$ to be the complex root of $\bar{K}^2$ that lies in the first quadrant. The constants C and D are easily determined by substituting (14) into (9). Outside the slab, $|y_2| > h$, equation (9) can be written in the form

$$< u^{\mathrm{T}} >_\infty (y_2) = u_0 T \exp(iky_2\cos\theta), \quad y_2 > h, \tag{16}$$

$$< u^{\mathrm{T}} >_\infty (y_2) = u_0 \exp(iky_2\cos\theta) + u_0 R\exp(-iky_2\cos\theta), \quad y_2 < -h. \tag{17}$$

In (16) and (17), the transmission coefficient T and the reflection coefficient R are given by

$$T = 4kK\cos\theta/\Delta\,, \tag{18}$$

$$R = (K^2 - k^2\cos^2\theta)[\exp(-2iKh) - \exp(2iKh)]/\Delta\,, \tag{19}$$

$$\Delta = (K + k\cos\theta)^2 \exp[-2i(K - k\cos\theta)h] - (K - k\cos\theta)^2 \exp[2i(K + k\cos\theta)h]\,. \tag{20}$$

It follows from (14), (15), and (6) that there is a forward wave and a backward wave inside the cracked region. Both waves are attenuated and have velocity c such that

$$c = c_T/V(\theta)\,, \qquad V(\theta) = \left[\sin^2\theta + \cos^2\theta(\mathrm{Re}\bar{K})^2\right]^{\frac{1}{2}}. \tag{21}$$

If $\tilde{\omega} = \omega a s_{\mathrm{T}}$ denotes the dimensionless frequency, and if the crack density $\epsilon = na^2$ is less than $1/\pi$, one can show from (10), (11), (12), (15), and (21) that

$$\frac{c}{c_{\mathrm{T}}} = \frac{(1 - \epsilon\pi)^{1/2}}{E^{1/2}} + O(\tilde{\omega}^2 \mathrm{Log}\tilde{\omega})\,, \quad E = 1 - \epsilon\pi\sin^2\theta\,, \quad (\epsilon < 1/\pi)\,, \quad \text{as } \tilde{\omega} \to 0\,. \tag{22}$$

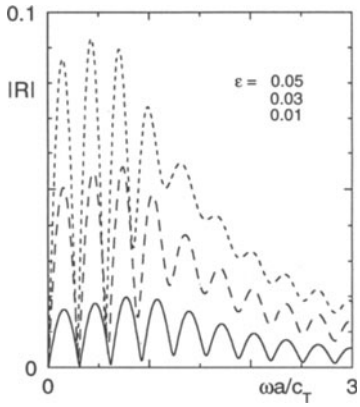

Figure 2. Modulus of the reflection coefficient versus the frequency for $h/a = 5$, $\epsilon = 0.01,\ 0.03,\ 0.05$, and normal incidence $\theta = 0$ degree.

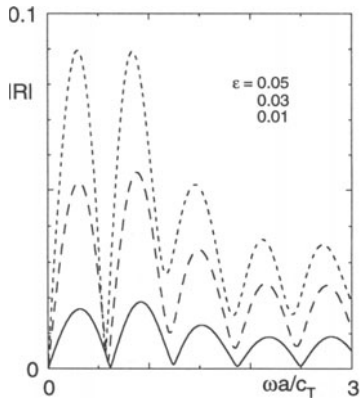

Figure 3. Modulus of the reflection coefficient versus the frequency for $h/a = 5$, $\epsilon = 0.01,\ 0.03,\ 0.05$, and incident angle $\theta = 60$ degrees.

The only assumption that is needed to obtain the formulas (18) and (19) for the transmission and reflection coefficients is Foldy's assumption. The two coefficients depend on frequency, crack length, crack density, slab thickness, incident angle, and on the speed of transverse waves in the uncracked solid.

NUMERICAL RESULTS

Numerical results are obtained by solving the integral equations (11) and (12) with a Gaussian method of approximation, as in [6, 7]. We evaluate successively the following quantities: *(i)* the function b; *(ii)* the number B of (10); *(iii)* the wavenumber K of (15); *(iv)* the coefficients T and R of (18) and (19).

Figure 2 $\{3, 4\}$ shows the modulus of the reflection coefficient versus the dimensionless frequency for incident angle $\theta = 0°$ $\{\theta = 60°,\ 75°\}$, crack densities $\epsilon = 0.01, 0.03, 0.05$ and slab thickness $h/a = 5$. The reflection is small (less than 0.1) in the three figures. At $\tilde{\omega} = 0$, the value of $|R|$ is zero. As $\tilde{\omega}$ increases, the values of

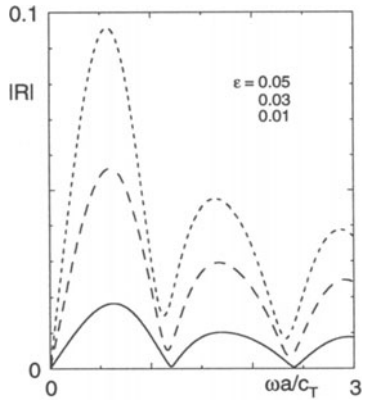

Figure 4. Modulus of the reflection coefficient versus the frequency for $h/a = 5$, $\epsilon = 0.01,\ 0.03,\ 0.05$, and incident angle $\theta = 75$ degrees.

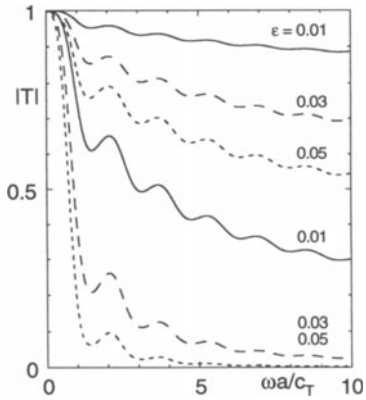

Figure 5. Modulus of the transmission coefficient versus the frequency for $h/a = 3$ (three upper curves) and $h/a = 30$ (three lower curves), $\epsilon = 0.01,\ 0.03,\ 0.05$, and incident angle $\theta = 60$ degrees.

$|R|$ have cyclic variations caused by interference phenomena inside the cracked region. The first minimum on each of the curves occurs approximately when the incident wave has a wavelength of $4h\cos\theta$. The following minima occur approximately at wavelengths that are integer multiples of $4h\cos\theta$.

Figure 5 shows the modulus of the transmission coefficient versus the dimensionless frequency for incident angle $\theta = 60°$, crack densities $\epsilon = 0.01, 0.03, 0.05$ and slab thicknesses $h/a = 3,\ 30$. At $\tilde{\omega} = 0$, the value of $|T|$ is 1. As $\tilde{\omega}$ increases, the values of $|T|$ decrease. The decrease is steeper when the crack density ϵ is larger, when the thickness h/a is larger and (as shown in [6, 7]) when the incident angle θ is closer to 0°. As the frequency $\tilde{\omega}$ becomes large, the values of $|T|$ approach the limit $\exp(-4\epsilon\, h/a)$ independently of the angle of incidence θ.

STATIC APPROXIMATION

When the slab of width $2h$ in Fig. 1, instead of being cracked, is made of a homogeneous elastic solid different from the surrounding solid, it is not difficult to

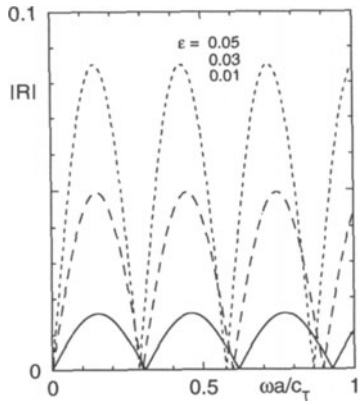

Figure 6. Modulus of the reflection coefficient versus the frequency for $h/a = 5$, $\epsilon = 0.01,\ 0.03,\ 0.05,$ and normal incidence $\theta = 0$ degree; static equivalent slab.

calculate the transmission T and reflection R on either side of the slab. If ρ, c_{T}, s_{T} $\{\rho,\ c,\ s\}$ denote the mass density, transverse-wave speed and slowness outside $\{$inside$\}$ the homogeneous slab, and if there is a perfect bonding between the two solids at $y_2 = \pm h$, one finds that the moduli of T and R are given by

$$|T| = 2(\rho c_{\mathrm{T}}\ \cos\theta)\ (\rho c\ \cos\theta_s)/\Omega\ , \tag{23}$$

$$|R| = \left|(\rho c_{\mathrm{T}}\ \cos\theta)^2 - (\rho c\ \cos\theta_s)^2\right|\ |\Phi|/\Omega\ , \tag{24}$$

$$\Omega^2 = \left[(\rho c_{\mathrm{T}}\ \cos\theta)^2 - (\rho c\ \cos\theta_s)^2\right]^2\ \Phi^2 + 4\,(\rho c_{\mathrm{T}}\ \cos\theta)^2\ (\rho c\ \cos\theta_s)^2\ , \tag{25}$$

$$\Phi = \sin\left[2\omega s_{\mathrm{T}} h\,(s\ \cos\theta_{\mathrm{S}}/s_{\mathrm{T}})\right]\ , \qquad s_{\mathrm{T}}\ \sin\theta = s\ \sin\theta_{\mathrm{S}}\ . \tag{26}$$

In (23) - (26), θ_{S} denotes the refracted angle in the slab. Observe that both $|T|$ and $|R|$ are periodic functions of period π with respect to the variable $2\omega sh\ \cos\theta_{\mathrm{S}}$. The transmission $|T|$ oscillates between 1 and a minimum value less than 1, and the reflection $|R|$ oscillates between zero and a maximum value $|R|_m$ less than 1.

Now let the homogeneous slab of thickness $2h$ be made of the static equivalent solid corresponding to the limit $\tilde{\omega} = 0$ of (22). Then, using (22), (24) and (26), one finds that

$$\rho c\ \cos\theta_{\mathrm{S}} = \rho c_{\mathrm{T}}\ \cos\theta\,(1-\epsilon\pi)^{\frac{1}{2}}/E\ , \qquad s\ \cos\ \theta_s/s_{\mathrm{T}} = \cos\ \theta/(1-\epsilon\pi)^{\frac{1}{2}}\ , \tag{27}$$

$$|R|_m = |E^2 - 1 + \epsilon\pi|/(E^2 + 1 - \epsilon\pi)\,, \qquad (\epsilon < 1/\pi)\,. \tag{28}$$

Choosing $\theta = 0°$, $h/a = 5$, and $\epsilon = 0.01,\ 0.03,\ 0.05,$ one finds that the reflection $|R|$ of (24) and (27) versus $\tilde{\omega} = \omega a s_{\mathrm{T}}$ has the form shown in Fig. 6.

Observe that the curves of Fig. 2 are in good agreement with those of Fig. 6 for low frequencies $\tilde{\omega} < 0.8$. For higher frequencies, the approximate reflection of Fig. 6 does not decay toward zero as does the reflection of Fig. 2; further, it has

cyclic local minima that always take zero values, whereas the corresponding values are non-zero in Fig. 2.

For $\theta = 60°$, $h/a = 5$, and $\epsilon = 0.01$, 0.03, 0.05, respectively, the maximum values of the reflection given by (28) are 0.0079, 0.0238, 0.0399. These values are less than half those of the first local maxima that occur at about $\tilde{\omega} = \pi/10$ in Fig. 3. Thus, the approximate formulas (24) and (27) do not give a good estimate of the peak reflections for oblique incidence; they still give, however, a good estimate of the frequency locations corresponding to the cyclic local minima.

ACKNOWLEDGEMENTS

This material is based in part upon work supported by the Texas Advanced Technology Program under Grant No. 003604–004. The authors thank Professor V.K. Kinra for helpful discussions.

REFERENCES

1. M. Kikuchi, "Dispersion and Attenuation of Elastic Waves due to Multiple Scattering from Cracks," Physics of the Earth and Planetary Interiors **27**, 100–105 (1981).
2. J. Kawahara and T. Yamashita, "Scattering of Elastic Waves by a Fracture Zone Containing Randomly Distributed Cracks," Pure and Applied Geophysics **139**, 121–144 (1992).
3. Ch. Zhang and D. Gross, "Wave Attenuation and Dispersion in Randomly Cracked Solids – I. Slit Cracks," International Journal of Engineering Science **31**, 841–858 (1993).
4. V.P. Smyshlyaev, J.R. Willis, and F.J. Sabina, "Self-Consistent Analysis of Waves in a Matrix-Inclusion Composite – III. A Matrix Containing Cracks," Journal of the Mechanics and Physics of Solids **41**, 1809–1824 (1993).
5. A.S. Eriksson, A. Boström, and S.K. Datta, "Ultrasonic Wave Propagation Through a Cracked Solid," Wave Motion **22**, 297–310 (1995).
6. Y.C. Angel and Y.K. Koba, "Complex-Valued Wavenumber, Reflection, and Transmission in an Elastic Solid Containing a Cracked Slab Region," International Journal of Solids and Structures, in press.
7. Y.C. Angel and A. Bolshakov, "Oblique Coherent Waves Inside and Outside a Randomly Cracked Elastic Solid," Journal of the Acoustical Society of America, in press.